ISSN No: 2348-4845
International Journal & Magazine of Engineering, Technology, Management and Research
A Peer Reviewed Open Access International Journal

Outline and Control of a Bidirectional Resonant Dc–Dc Converter and Multilevel Inverter at Load Side-Dc/Ac

D.Pavan Kumar
M.Tech Student,
Malla Reddy Engineering College.

Ch.Naveen Kumar
Assistant Professor,
Malla Reddy Engineering College.

Abstract:

In this paper, a bidirectional dc–dc converter and multilevel inverter at burden side-dc/air conditioning is proposed for the car motor/battery half breed force generators. The two-stage bidirectional converter utilizing a settled recurrence arrangement stacked thunderous converter is intended to be equipped for working under zero-present exchanging turn-on and turn-off paying little heed to voltage and burden variety, and consequently its attractive segments and EMI channels can be improved. An awesome piece of this paper is given to indicate nontraditional applications fueled by multilevel converters and how multilevel converters are turning into an empowering innovation in numerous mechanical divisions. Additionally, another self-ruling and consistent bidirectional voltage control system that joins two individual controllers for low-voltage side control and high-voltage side control by presenting a variable current limiter is proposed to give continuous energy to basic air conditioning loads and decrease the span of the dc transport capacitor and the move time. At last, some future patterns and difficulties in the further improvement of this innovation are talked about to inspire future commitments that address open issues and investigate new potential oututs.

I.INTRODUCTION:

Increase in demand of Electricity leads to the use of renewable energy sources such as solar, wind etc. In case of solar energy is harnessed in the form of dc. This DC is converted into AC and fed to grid or ac loads. In recent years there was increase in demand for multilevel power conversion. Research has involved the introduction of novel converter topologies and unique modulation strategies. However, the most recently used inverter topologies, are cascade inverter, neutral-point clamped (NPC) inverter, and flying capacitor inverter. Our proposed topology consists of level module and H-Bridge inverter and they are connected in parallel. Proposed topology is symmetric topology since the values across all the DC sources are same.

However, there are asymmetrical topologies which require different voltage sources. This criterion needs to arrange dc power supplies according to a specific relation between the supplies. Difference in ratings of the switches in the topology is also a major drawback of the topology. This paper presents an overview of a new multilevel inverter topology named reversing voltage (RV). This topology requires less number of components compared to conventional topologies. It is also more efficient since the inverter has a component which operates the switching power devices at line frequency. Therefore, there is no need for all switches to work in high frequency which leads to simpler and more reliable control of the inverter.

The proposed two-stage BDC consists of a non-isolated converter and a fixed-frequency SRC. The SRC is designed to be capable of operating under ZCS turn-on and turn-off regardless of voltage and load variation in both forward and reverse operation. A method of adjusting dead time of the SRC will be presented to minimize the turn-on switching losses associated with energy stored in MOSFET's output capacitances during the ZCS turn-on process. Also, a new autonomous and seamless bidirectional voltage control strategy is proposed to provide uninterrupted power to the critical ac loads and reduce the size of the dc bus capacitor and the transition time.

Petroleum resources across the world is depleting at a high rate due to the large dependency of the transportation sector on petroleum as the primary fuel. Also due to this, there is a vast greenhouse gas emission that is degrading the quality of air and causing harm to life and environment. This has aroused a tremendous interest for the design of the vehicles with lesser or no dependency on the petroleum resources. And therefore the alternate propulsion technologies have been increasingly pursued by the automobile industries and this has led to the increased development rate of the of the Hybrid Electric Vehicle (HEV) technology in the past two decades. The first HEV car was introduced during 1900 by Lohner Coach Factory, which was driven by a hub

ISSN No: 2348-4845
International Journal & Magazine of Engineering, Technology, Management and Research
A Peer Reviewed Open Access International Journal

motor powered by the generator run through a gasoline engine with a small battery for reliability. But since then due to the better development in the ICE technologies and the cheaper petroleum prices made the ICE run vehicle a better option than a HEV. Therefore the growth of the HEV technologies remained almost stagnant until recent past two decades when the petroleum prices started rising due to their limited availability and greater consumption as well as because of the degrading atmospheric and environmental conditions because of the emissions due to hydrocarbon combustion . An HEV unlike conventional vehicle, which depends solely on the ICE engine for the traction power, utilizes electrical energy storage in combination with the ICE to provide the required traction power. Thus it facilitates the improvement in the energy 2 1.3 Contribution of the Thesis conversion of the vehicle thereby increasing the efficiency and drivability and at the same time reducing the emissions. Furthermore the integration of the electrical storage system also makes the provision for the regeneration during braking which can further boost up the efficiency of the overall system.

II.MULTILEVEL TOPOLOGIES OVERVIEW:

For completeness and better understanding of the advances in multilevel technology, it is necessary to cover classic multilevel converter topologies. However, in order to focus the content of this paper on the most recent advances and ongoing research lines, well-established topologies will only be briefly introduced and referred to existing literature. In the following, classic topologies will be referred to those that have extensively been analyzed and documented and have been commercialized and used in practical applications for more than a decade. Multilevel converter technology started with the introduction of the multilevel stepped waveform concept with a series-connected H-bridge, which is also known as cascaded H-Bridge converter, in the late 1960s [27]. This was closely followed by low-power development of an FC topology the same year [28]. Finally, in the late 1970s, the diode-clamped converter (DCC) [29] was first introduced. The DCC concept evolved into the three-level NPC (3L-NPC) converter we know today as it was proposed in [30]–[32] and can be considered as the first real multilevel power converter for medium-voltage applications. Later, the CHB would be reintroduced in the late 1980s [33], although it would reach more industrial relevance in the mid-1990s [34].

In the same way, the early concept of the FC circuit introduced for low power in the 1960s developed into the medium-voltage multilevel converter topology we know today in the early 1990s [35]. Through the years, the FC has also been reported as the imbricated-cell and multicell converter. (The latter is also a name used for the CHB since both are modular and made by interconnection of power cells.) These three multilevel converter topologies could be considered now as the classic or traditional multilevel topologies that first made it into real industrial products during the last two decades. The power circuits of a single-phase leg of these three topologies are shown in Fig. 1, featuring the corresponding commonly used semiconductor device. These converters are commercialized by several manufacturers in the field [11]–[26], offering different power ratings, front-end configurations, cooling systems, semiconductor devices, and control schemes, among other technical specifications. The most relevant parameters and ratings for each of these classic topologies are listed in Table I. The parameters for each category are given for the different manufacturers, whose corresponding reference is given at the bottom of the table. As can be observed from the table, the 3L-NPC and the CHB are the most popular multilevel topologies used in the industry..

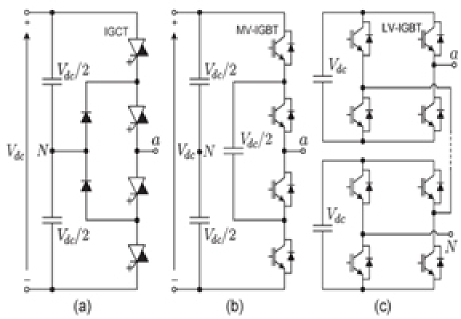

Fig. 1. Classic multilevel converter topologies (with only one phase shown). (a) 3L-NPC featuring IGCTs. (b) Three-level FC featuring MV-IGBTs. (c) Five-level CHB featuring LV-IGBTs.

II. PROPOSED BDC:

The proposed BDC consists of two power conversion stages: a non-isolated converter and a fixed-frequency SRC, as shown in Fig. 2. Since the SRC is operated at fixed frequency and fixed duty, all components can be designed with minimum voltage and current rating. The non-isolated converter is operated to regulate either high side voltage VH or low side voltage VL according to the demanded load power and availability of the engine generator.

ISSN No: 2348-4845
International Journal & Magazine of Engineering, Technology, Management and Research
A Peer Reviewed Open Access International Journal

Figs. 3 and 4 show key waveforms and operation states of the proposed SRC, respectively. The angular resonant frequency of the resonant circuit can be expressed as

$\omega r = 2\pi fr = 1/\sqrt{Lr} \cdot Cr$ (1)

where resonant inductance and resonant capacitance can be determined, respectively, by

$$L_r = L_{kp} + \frac{L_m \cdot n^2 L_{ks}}{L_m + n^2 L_{ks}} \quad (2)$$

$$Cr = Cr1 + Cr2 \, . \quad (3)$$

It is seen from Figs. 3 and 4 that the low side current iL (=iSL2) at Mode I(t0−t1) becomes purely sinusoidal if the on-time duty cycle is selected such that DTs = 0.5/fr . Then it can be expressed as

$$i_L(t) = \frac{\pi I_{L,\mathrm{dc}}}{2} \sin \omega_r t \quad . (4)$$

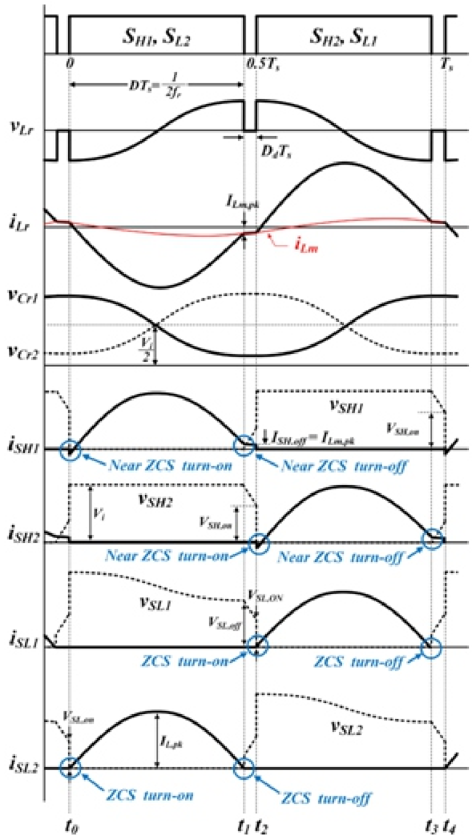

Fig. 3. Key waveforms of the proposed SRC.

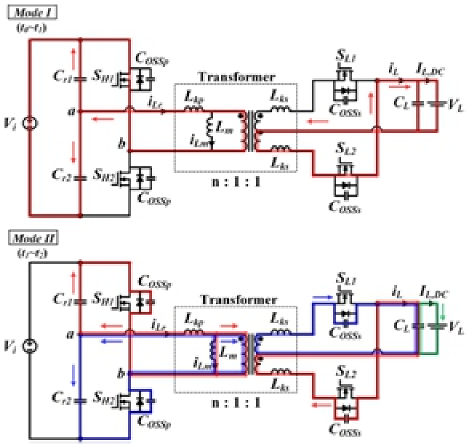

Fig. 4. Operation states of the proposed SRC. Also, voltage across Lm can be expressed as

$$v_{Lm}(t) = -n\left(V_L + L_{ks}\frac{di_L}{dt}\right) \quad (5)$$

Therefore, from (4) and (5), the magnetizing current at Mode I (t0−t1) can be expressed using iLm(t0) = – iLm(t1) by iLm(t) = nπVL

$$i_{Lm}(t) = \frac{n\pi V_L}{2\omega_r L_m} - \frac{nV_L}{L_m}t + \left(\frac{n\pi L_{ks} I_{L,dc}}{2L_m}\right)\sin \omega_r t \quad . (6)$$

The resonant current can then be obtained using (4) and (6) by

$$i_{Lr}(t) = \frac{n\pi V_L}{2\omega_r L_m} - \frac{nV_L}{L_m}t + \left(\frac{n\pi L_{ks} I_{L,dc}}{2L_m} - \frac{\pi I_{L,dc}}{2n}\right)\sin \omega_r t \quad (7)$$

Neglecting voltage oscillation after turning ON of SL2 , the voltage across low side switch SL1 at Mode I (t0−t1) is expressed as

$$v_{\mathrm{SL1}}(t) = 2V_L + L_{ks}\frac{di_L}{dt} \quad . (8)$$

The turn-off voltage of low side switch can be obtained by

$$V_{\mathrm{SL,off}} = 2V_L - \frac{\pi \omega_r L_{ks} I_{L,\mathrm{dc}}}{2} \quad (9)$$

It should be noted that VSL,off should be greater than zero for the proposed operation. Therefore, from (4) and (9) the secondary side leakage inductance should be limited such as

ISSN No: 2348-4845
International Journal & Magazine of Engineering, Technology, Management and Research
A Peer Reviewed Open Access International Journal

$$L_{ks} < \frac{4V_L}{\pi\omega_r I_{L,\mathrm{dc}}} \quad (10)$$

Switch SH1 is turned OFF at t1 , and turn-off current of the high side switch, ISH,off , becomes equal to the peak magnetizing current ILm,pk . Since Lm is made very large in the proposed SRC, ILm,pk is very small, resulting in negligible switch turnoff losses.During Mode II, the output capacitors of SH1 and SH2 are charged and discharged, respectively by ILm,pk, as shown in Fig. 3. The charging and discharging operation may not be completed at the end of Mode II if ILm,pk is not sufficiently large, which may lead to a nonzero turn-on voltage of high and low side switches. The turn-on voltages of the high and low side switches can be determined respectively by

$$V_{\mathrm{SH,on}} = v_{\mathrm{SH2}}(t_2) = V_i - \frac{n^2 I_{Lm,pk} D_d T_s}{2n^2 C_{\mathrm{OSSp}} + 2C_{\mathrm{OSSs}}} \quad (11)$$

$$V_{\mathrm{SL,on}} = v_{\mathrm{SL1}}(t_2) = \frac{4V_L - \pi\omega_r L_{ks} I_{L,\mathrm{dc}}}{2} - \frac{n I_{Lm,pk} D_d T_s}{2n^2 C_{\mathrm{OSSp}} + 2C_{\mathrm{OSSs}}} \quad (12)$$

Note that SH2 and SL1 are turned ON with ZCS, but there exists turn-on losses of high- and low side switches associated with energy stored in MOSFET's output capacitances as follows [18], [19]:

$$P_{\mathrm{SH,loss(on)}} = 0.5 C_{\mathrm{OSSp}} V_{\mathrm{SH,on}}^2 f_s \quad (13)$$

$$P_{\mathrm{SL,loss(on)}} = 0.5 C_{\mathrm{OSSs}} V_{\mathrm{SL,on}}^2 f_s \quad (14)$$

However, the turn-on losses of the switches may be considerable in the high-voltage application. The turn-on loss PSL, loss (on) of the low side switch is negligible since VSL, on is small in this low voltage application, and the turn-on loss PSH, loss(on) of the high side switch is also small due to the two-stage configuration.In the proposed SRC, PSH, loss (on) can further be reduced by increasing DdTs and, in turn, decreasing VSH on, as shown in Fig. 3.

However, increasing DdTs may cause increased current ratings and undesired resonance, and hence it should be properly chosen. Therefore, it is noted that both turn-off and turn-on switching losses of the proposed SRC are made negligible in this application. In the conventional frequency-controlled SRC, in general, resonant inductance Lr should be made large to reduce the switching frequency range.

In the proposed SRC, on the contrary, Lr is chosen to be small since the SRC is not used for regulation, resulting in a very small gain variation according to load variation in both the charging and discharging modes, as shown in Fig. 5. This also allows Lr to be easily embedded in the transformer. Also, the proposed SRC is able to achieve ZCS turn-on and turn-off of the switch without regard to voltage or load variation by choosing the resonant frequency fr as follows:

$$f_r = \frac{1}{2D} f_{s1} = \frac{1}{1 - 2D_d} f_{s1} \quad (15)$$

Furthermore, small Lr leads to less sensitive resonant component tolerances, eliminating the voltage regulation issues and saturation problem of magnetic devices that were introduced in the conventional frequency-controlled SRC [20], [21]. In order to demonstrate the impact of component tolerances on the voltage gain and the soft switching characteristics, the following assumptions are made for the component value:
1) resonant inductance Lr : ±10%;
2) resonant capacitance Cr : ±10%.
The effective resonant frequency is defined by

$$f_{r(\mathrm{eff})} = \frac{1}{2\pi\sqrt{L_{r(\mathrm{eff})} \cdot C_{r(\mathrm{eff})}}} \quad (16)$$

where Lr(eff) and Cr(eff) are effective resonant inductance and capacitance, respectively, reflecting component tolerances. As shown in Fig. 6, the variation in voltage gain of the proposed SRC according the resonant component tolerances is negligible [20]. When fr(eff) > fr , the SRC behaves like region II operation of LLC converter and is turned OFF with the magnetizing current at turn-off instant. Note that the proposed SRC can be said to be turned OFF with near ZCS since the magnetizing current of the proposed converter is very small compared to LLC converter due to the larger magnetizing inductance. When fr(eff) < fr , the SRC is operated under inductive region and turned OFF with hard switching.

III. PROPOSED CONTROL STRATEGY:

The high side dc bus is regulated to either 400 V by the ac–dc converter or 380 V by the BDC, respectively, according to the condition of VH . The conventional control of the BDC is in general realized with the two individual controllers of VL control for battery charging and VH control for battery discharging, and

ISSN No: 2348-4845
International Journal & Magazine of Engineering, Technology, Management and Research
A Peer Reviewed Open Access International Journal

therefore may not be able to avoid large transient during the transition from VL control to VH control of the BDC.

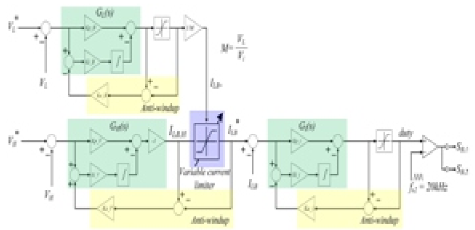

Fig. 7. Control block diagram of the proposed battery charger.

In this paper, a new autonomous and seamless bidirectional voltage control strategy, as shown in Fig. 7, is proposed to provide uninterrupted power to the critical ac loads and reduce the size of the dc bus capacitor. The two outer loop voltage controllers for VL control and VH control are combined by variable current limiter (VCL) whose output ILB is automatically selected to be either ILB,H, the output of the high side voltage controller, or ILB+, the positive limit of VCL which varies with the output of the low side voltage controller. This makes it possible to share inner-loop current controller, resulting in autonomous and seamless transition from VL control (charging mode) to VH control (discharging mode), and vice versa.The peak values of the positive and negative limits, ILB−,pk and ILB+,pk , of the VCL are determined by

$$I_{\mathrm{LB}+,pk} = I_{\mathrm{LB}-,pk} = \frac{P_i}{V_i} \quad .(17)$$

According to C-rate of the battery used, ILB+,pk may be chosen smaller than (17). ILB+ varies with magnitude of VL, while ILB− is always fixed at ILB−,pk . The anti windup is used to prevent the saturation of the controllers. For the sake of simplicity, it is assumed that the dc-load is constant and all the power losses of the ac–dc converter, the dc–ac inverter, and the BDC in Fig. 1 are neglected.

IV. SIMULATION RESULTS:

Simulation is performed using MATLAB/SIMULINK software. Simulink liabrary files include inbuilt models of many electrical and electronics components and devices such as diodes, MOSFETS, capacitors, inductors, motors, power supplies and so on. The circuit components are connected as per design without error, parameters of all components are configured as per requirement and simulation is performed.

CIRCUIT

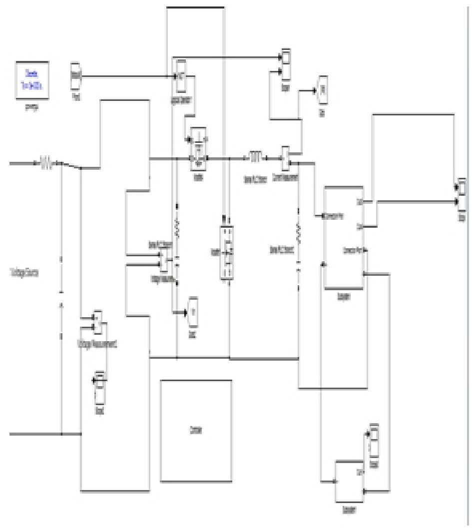

CONTROLLER CIRCUIT’

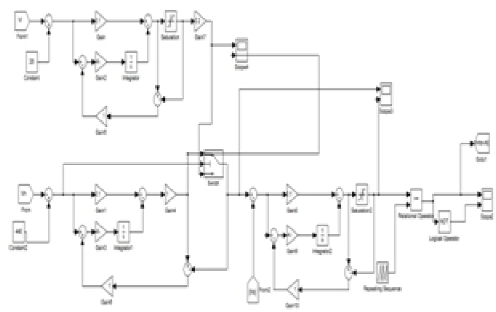

SEVEN LEVEL INVERTER OUTPUT

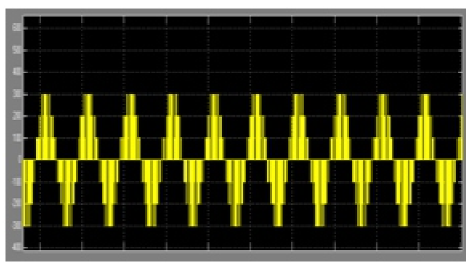

DC INPUT

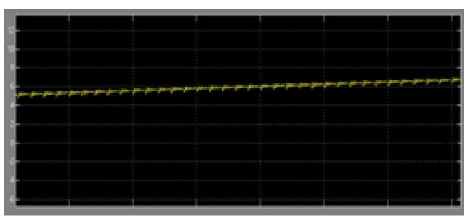

ISSN No: 2348-4845
International Journal & Magazine of Engineering, Technology, Management and Research
A Peer Reviewed Open Access International Journal

BATTERY VOLTAGE AND CURRENT

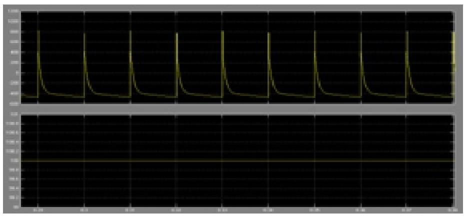

V. CONCLUSION:

In this paper, a bidirectional dc–dc converter and multilevel inverter at burden side-dc/air conditioning is proposed for the car motor/battery half breed force generators. The inverter utilized here is a seven level voltage source inverter. Performance of this system is tested using MATLAB/simulink

REFERENCES:

[1] P. Famouri, W. R. Cawthorne, N. Clark, S. Nandkumar, C. Atkinson, R. Atkinson, T. McDaniel, and S. Petreanu, "Design and testing of a novel linear alternator and engine system for remote electrical power generation," in Proc. IEEE Power Eng. Soc. Winter Meeting, Jan. 31–Feb. 4, 1999, pp. 108–112.

[2] Z. Chen andY. Hu, "Ahybrid generation system using variable speed wind turbines and diesel units," in Proc. IEEE 29th Annu. Conf. Ind. Electron. Soc., Nov. 2–6, 2003, pp. 2729–2734.

[3] E.Muljadi and T. J. Bialasiewicz, "Hybrid power system with a controlled energy storage," in Proc. IEEE 29th Annu. Conf. Ind. Electron. Soc., Nov. 2–6, 2003, pp. 1296–1301.

[4] L. Wang and D. Lee, "Load-tracking performance of an autonomous SOFC-based hybrid power generation energy storage system," IEEE Trans. Energy Convers., vol. 25, no. 1, pp. 128–139, Mar. 2010.

[5] D. Kim and S. Choi, "Load balancing with mobile base stations in tactical information communication networks," in Proc. IEEE Wireless Commun. Netw. Conf., Mar. 28–31, 2011, pp. 28–31.

[6] H. Wen, X. Wen, J. Liu, X. Guo, and F. Zhao, "A low-inductance highfrequency film capacitor for electric vehicles," in Proc. Int. Conf. Electr. Mach. Syst., Oct. 8–11, 2007, pp. 2046–2050.

[7] Y. X. Qin, H. S. H. Chung, D. Y. Lin, and S. Y. R. Hui, "Current source ballast for high power lighting emitting diodes without electrolytic capacitor," in Proc. IEEE 34th Annu. Conf. Ind. Electron., Nov. 10–13, 2008, pp. 1968–1973.

[8] J. Kim and S. Sul, "Resonant link bidirectional power converter. Part II—Application to bidirectional AC moto r drive without electrolytic capacitor," IEEE Trans. Ind. Appl., vol. 10, no. 4, pp. 485–493, Jul. 1995.

[9] H. Chae, H. Moon, and J. Lee, "On-board battery charger for PHEV without high-voltage electrolytic capacitor," Electron. Lett., vol. 46, pp. 1691– 1692, Dec. 2010.

[10] L. Rongyuan, A. Pottharst, N. Frohleke, and J. Bocker, "Analysis and design of improved isolated full-bridge bidirectional DC–DC converter," in Proc. IEEE 35th Annu. Power Electron. Spec. Conf., Jun. 20–25, 2004, pp. 521–526.

[11] G. Ma, W. Qu, G. Yu, Y. Liu, N. Liang, and W. Li, "A zero-voltageswitching bidirectional DC–DC converter with state analysis and softswitching- oriented design consideration," IEEE Trans. Ind. Electron.,vol. 56, no. 6, pp. 2174–2184, Jun. 2009.

[12] R. W. De Doncker, D. M. Divan, and M. H. Kheraluwala, "A three-phase soft-switched high-power density DC/DC converter for high-power applications," IEEE Trans. Ind. Appl., vol. 27, no. 1, pp. 63–73, Jan. /Feb. 1991.